Photoemission from Azobenzene Alkanethiol Self-Assembled Monolayers

R. Weber, B. Winter,* and I. V. Hertel

Max-Born-Institut für Nichtlineare Optik und Kurzzeitspektroskopie, Max-Born-Str. 2A, D-12489 Berlin, Germany

B. Stiller, S. Schrader, and L. Brehmer

Universität Potsdam, Institut für Physik, Lehrstuhl Physik Kondensierter Materie, Am Neuen Palais 10, D-14469 Potsdam, Germany

N. Koch

Institut für Physik, Physik von Makromolekülen, Humboldt-Universität zu Berlin, D-12489 Berlin, Germany

Received: December 31, 2002; In Final Form: March 26, 2003

Photoelectron spectra were measured for films of self-assembled azobenzene-terminated alkanethiol monolayers on gold using synchrotron radiation. The azobenzene was substituted either by CF_3 or CH_3 in the para position. As a result of the orientational order of the molecules within the films, as indicated by the pronounced angle dependence of the photoemission spectra, it is possible to identify laser-induced optical switching of the molecules using combined laser and synchrotron pulses. Molecular switching, i.e., photoisomerization, is recognized by relative intensity changes of the photoemission peaks and also by spectral shifts to higher binding energies. The latter result from a change of the molecular dipole moment associated with the trans-cis laser-induced photoisomerization of the azobenzene-CF_3 group.

1. Introduction

Self-assembled monolayers (SAMs) terminated by azobenzene functional groups are of interest as a result of an efficient trans−cis−trans reversible photoisomerization process.[1−4] Their electronic and thermal properties make them promising molecular moieties for optical molecular switches, optoelectronic and nonlinear optical applications, as well as for sensors.[1−4] Combined with the potential of SAMs to modify surfaces, such azobenzene functionalized systems represent invaluable model systems of biological and technological interest. SAMs of alkanethiols are among the most intensively studied systems as they can be easily bound to several relatively inert metal surfaces (e.g., Au, Ag) via reaction with the thiol group.[5,6,7]

To understand the physical and chemical processes occurring in such systems, it is essential to characterize their electronic structure. In the case of azobenzene end-groups, one would want to correlate the molecules' structural changes upon photoisomerization to the subsequent electronic structural changes. This information is expected to be useful for a basic understanding of the isomerization process. Currently, however, photoelectron spectroscopic data from azobenzene-containing thin films are rare.[8,9]

The present study is concerned with the photoemission from azobenzene derivatives functionalized either with CF_3 or with CH_3 in the para position, and with oxyalkanethiol in the para' position, which allowed the formation of self-assembled monolayers grafted onto gold. The purpose is to assign spectral features to individual molecular orbitals, and to evaluate the possibility to reliably distinguish cis and trans azobenzene isomers by their valence photoemission spectra. The combined laser and synchrotron irradiation experiments presented are aimed to investigate the effect of 360 nm laser light on the electronic structure of azobenzene-CF_3-terminated alkanethiol SAMs. Exposure by 360 nm photons is known to transform the azobenzene group from the trans to the cis configuration. This process is reversible, and irradiation with 450 nm light, corresponding to the absorption maximum for the reverse transformation, almost entirely reestablishes the initial film configuration.[2−4] This back-and-forth switching has been recently demonstrated by directly measuring the surface potential change over several switching cycles using the Kelvin probe method.[4] The difference in surface potential between the two isomers is related to the net change of the molecular dipole moment (normal component with respect to the surface). Hence, the presence of a polar tail group, such as CF_3, serves as a sensor for isomerization. Notice that the nonsubstituted molecule has no permanent dipole moment. In photoemission surface dipoles give rise to spectral shifts associated with changes of the samples' work function.

The optical switching of azobenzene requires both a free volume in the films and a suitable spacer in order to reduce the metal substrate−azobenzene interaction.[2−4] As the footprint area in the cis configuration is more than twice as large as for trans, larger free volume allows for more efficient photoisomerization in the film.[2] Therefore, experiments have been performed for azobenzene alkanethiol systems with lower chromophore surface-density as well. The latter contained azobenzene-CF_3-terminated decanethiol and nonsubstituted dodecanethiol at a ratio of about 1:2.

Only subtle changes in the electronic structure can be expected since no breaking of bonds or the formation of new bonds is involved in the isomerization process. Any systematic

* Corresponding author. E-mail: bwinter@mbi-berlin.de.

10.1021/jp0226681 CCC: $25.00
Published on Web 07/18/2003

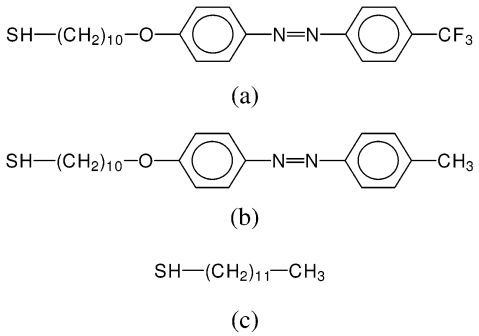

Figure 1. Chemical structure of the alkylthiols investigated: (a) azobenzene-CF_3- terminated alkanethiol; (b) azobenzene-CH_3-terminated alkanethiol; (c) dodecanethiol.

photoemission study that intends to follow photoisomerization processes in situ requires to carefully examine possible effects of the actual probe pulse, i.e., ultraviolet synchrotron light in the present case. High-energy synchrotron photons might induce processes similar to those initiated by lower energy laser radiation.

2. Experimental Section

2.1. Materials. As a result of the molecular symmetry, an isolated azobenzene group has no dipole moment in the trans state. Only an asymmetric substitution at the terminal positions of azobenzene leads to a permanent molecular dipole moment. For this reason, an azobenzene unit with a trifluoromethyl (CF_3) tail-group attached to the outer ring in the para position has been synthesized.[3,4] The resulting structure is 10-[4-(4-trifluoromethyl-phenylazo)-phenyl]-decane-1-thiol (Figure 1a).

Fluorination was a three-step process. First, 4-trifluoromethylaniline was diazotenized and coupled with phenol to give 4-trifluoromethyl-4′-hydroxy azobenzene. This was followed by alkylation with α,ω-dibromoalkylenes to the respective bromides. Both steps are very similar to the procedure described earlier.[10] The resulting compounds were converted into the corresponding thiols as described elsewhere.[3,4] For comparison also the analogous compound with methyl (CH_3)-terminated azobenzene (10-(4-*p*-tolylazo-phenyl)-decane-1-thiol) has been synthesized (Figure 1b), and dodecanethiol (dodecane-1-thiol) (Figure 1c) was used as received (Aldrich). The obtained thiol compounds were purified by recrystallization from ethanol and finally analyzed by elementary analysis, IR, and NMR spectroscopy.

2.2. Gold Substrate and Monolayer Preparation. Highly ordered monolayer azobenzene-terminated decanethiol films on gold have been prepared by the self-assembling technique.[3,4] The molecules are bound covalently to the gold through the thiol group. The methyl or the trifluoromethyl groups of the azobenzene ω-terminated alkyl chains are pointing away from the gold substrate as shown in Figure 2 for the case of CF_3-terminated azobenzene. The tilt angle of the alkyl moiety of azobenzene alkanethiols has been determined to be in the range of 14° to 30° relative to the substrate normal.[11−13] It is important to note that this still allows for an orientation of the azobenzene unit almost perpendicular to the substrate normal.[12,13] Gold films of 150 nm thickness were produced by thermal evaporation of gold onto a silicon wafer in high vacuum. The freshly prepared gold substrates were dipped into 10^{-3} M ethanol solutions of azobenzene alkanethiol for 24 h. Finally, the substrates were rinsed with pure ethanol to remove nongrafted molecules, and then dried in a nitrogen atmosphere. Similarly, azobenzene-CH_3-terminated decanethiols, pure dodecanethiols, and mixed films

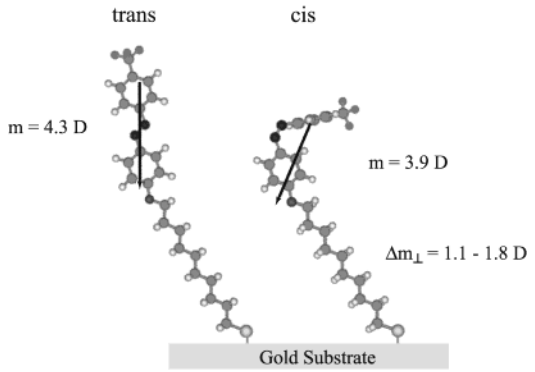

Figure 2. *Trans*- and *cis*-azobenzene-R terminated alkanethiols on a gold substrate; R = CF_3. The depicted inclination of the alkanethiol, by ca. 30° with respect to the surface normal, is assumed to be an upper limit. The respective absolute dipole moments, *m*, are indicated. $\Delta m_\perp$ denotes the change of the component of *m* perpendicular to the substrate surface, associated with the photoisomerization. Upper and lower limits are given (see text).

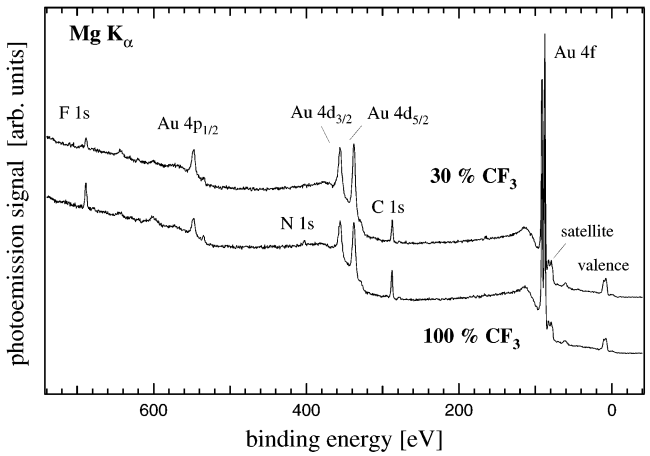

Figure 3. XPS survey spectra from two azobenzene-CF_3-terminated alkanethiol SAMs on Au using Mg K_α radiation; low-density 30% sample (top), 100% sample (bottom).

were obtained by dipping the freshly prepared gold substrate into a solution of the desired composition. Throughout this work, the two azobenzene-R-terminated decanethiol/Au systems will be referred to as CH_3azoC10 and CF_3azoC10, respectively, and C12 denotes the dodecanethiol/Au system. 30% CF_3azoC10 refers to a mixed SAM composed of 30% CF_3azoC10 and 70% C12. The film composition has been confirmed by X-ray photoemission spectroscopy (XPS) experiments. Survey XPS scans (using Mg K_α radiation) of the respective samples along with the peak assignment are displayed in Figure 3. Intensities are as measured since identical photon fluxes have been used. As expected, the F1s intensity for the high-density film is three times larger. The smaller intensities of the Au features in the 100% CF_3azoC10 film are consistent with the stronger attenuation of substrate electrons due to larger film thickness.

Sample quality was also controlled by atomic force microscopy (AFM);[14] all samples were stable in air. The switching ability of the films was confirmed by measuring the surface potential changes between the trans and cis configuration by means of the Kelvin probe method. These measurements were performed both before and after the photoemission experiments, and they agreed very well with published values on identically prepared samples.[3,4]

2.3. Photoelectron Spectroscopy. The photoemission experiments were performed at the undulator beamline (U125) of the Max-Born-Institut Berlin (MBI), Germany, at the Berlin Electron

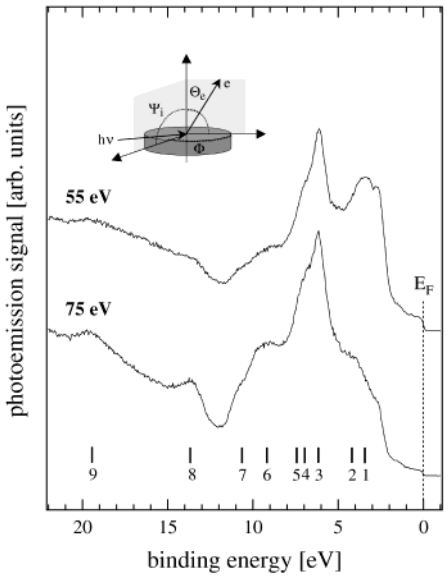

Figure 4. Normal emission photoelectron spectra from the dodecanethiol/Au SAM for $h\nu = 55$ eV (top) and 75 eV (bottom) at 83° photon incidence. The energy axis is with reference to the gold substrate Fermi level. For peak assignment, see text. The inset is a sketch of the experimental geometry used for photoemission.

Synchrotron facility (BESSY II). This beamline provides photon energies from 20 to 180 eV using two rotatable spherical gratings in combination with an adjustable planar mirror (VIA principle).[15,16] The experimental chamber, base pressure better than 2×10^{-10} mbar, is equipped with a spherical electron energy analyzer, a quadrupole mass spectrometer, a HeI resonance ultraviolet radiation source, and an X-ray source (Mg K_α). The energy resolution for 70 eV photons is about $E/dE = 10^4$ at ca. 5×10^{12} 1/s $\times$ 0.1A photon flux; however, much lower flux has been applied in the present study for minimizing possible sample damage. Photon fluxes have been adjusted by de-tuning the undulator gap. Photoelectrons were detected with a hemispherical electron energy analyzer (EA 125, Omicron) at 4° acceptance angle. The energy resolution of the spectrometer was typically 20 meV operating at 10 eV pass energy. Magnetic fields are suppressed to ca. 0.1 μT by a μ-metal layer inside the vacuum chamber. The angle of incidence of the synchrotron light was $\Psi_i = 83°$ with respect to the sample surface normal, and the photoelectrons were typically detected in normal emission (see inset Figure 4). The SAM samples were transferred into the main analysis chamber through a load-lock. They were mounted on a manipulator which allowed for sample rotation (azimuth Φ, tilt Ψ, polar Θ), and translation (x, y, z) in front of the energy analyzer. Samples can be cooled by liquid nitrogen and heated by electron impact. Angle-resolved photoemission spectra were recorded at electron emission angles Θ_e between 0° and 60° with the photon incidence angle Ψ_i fixed at 83° (see inset Figure 4). For this purpose the analyzer can be rotated away from the surface normal in the plane perpendicular to the synchrotron beam. All experiments were conducted at room temperature.

The MBI beamline, as part of a user facility for experiments with combined laser and synchrotron pulses, is equipped with a high-repetition rate Ti:sapphire laser system (MIRA, Coherent, Inc.) which is synchronized to the BESSY II master oscillator. The present measurements were performed during BESSY II multi bunch (500 MHz) operation, which corresponds to a synchrotron inter-pulse spacing of 2 ns. The laser repetition rate was set to 83.3 MHz, equivalent to 12 ns laser inter-pulse spacing. Hence, every sixth synchrotron pulse is synchronized with a laser pulse. This scheme has been previously applied,[16,17] and a detailed description of the laser-to-synchrotron pulse synchronization technique as well as its performance has been presented in ref 16. The laser pulses were 200 fs wide and the laser wavelength was tunable from about 720−900 nm and from 360 to 450 nm for the fundamental and second harmonic, respectively, at the respective output power of about 2 W and 500 mW. Both the laser and the synchrotron light were incident at the same angle Ψ_i but slightly different azimuth angle Φ_i. Spatial overlap of the two beams (800×200 μm^2 synchrotron focal size and ca. 1 mm^2 diameter of laser focus) was optimized using a thin fluorescent GdOS:Eu film sample mounted next to the actual sample. Maximum spatial overlap yielded the maximum compensation of the synchrotron-induced charging shift of the GdOS:Eu films of the photoemission spectrum. For determining the temporal overlap, or setting a desired time delay, the pulses from the two light sources have been detected by a fast ultraviolet sensitive photodiode (AXUV-HS3, IRD, Inc.) mounted on a precision manipulator. This allowed placing the photodiode at the nominal sample position.[16,17]

3. Results and Discussion

3.1. Spectral Assignment of Azobenzene-CF_3/CH_3-Terminated Alkanethiol Monolayers. Two characteristic valence photoemission (PE) spectra of the self-assembled dodecanethiol/Au system (C12) obtained for 55 and 75 eV excitation photon energy, respectively, are shown in Figure 4. Photon incidence was grazing, $\Psi_i = 83°$, and electron detection was at normal emission, $\Theta_e = 0°$ (see inset Figure 4 for notation). The polarization of the incident VUV (vacuum ultraviolet) photons was parallel to the substrate surface. The energy scale of the abscissa refers to binding energies relative to the Fermi-level (E_F) as determined on a polycrystalline gold sample. For clarity the spectra are vertically displaced. Since the overall spectral features in the figure are fully consistent with literature reports on comparable alkanethiol systems,[18,19] the same peak assignment is being used here. Accordingly, features labeled *8*, near 13.5 eV binding energy, and *9*, at about 20 eV binding energy (BE), are mainly attributed to the C2s valence emission from the alkane part of the molecules. Similarly, two peaks at 13.5 (18.5) and 17.3 (22.3) eV have been assigned to C2s emission for 1,9-nonanedithiol films.[18] The numbers in parentheses refer to the original BE values with respect to vacuum as given in the reference. The gold substrate work function was assumed to be 5.0 eV in order to allow a comparison to our BE values given relative to E_F. Additional nonresolved emission features exist between these two binding energies, near 16−18 eV. Likewise are three peaks contained in the C2s band in the case of 1-cyclobutyl-13-tridecanethiol films: 14.6 (19.6), 17.0 (22.0), and 20.3 (25.3) eV. Peaks *7*, *6*, *5*, *4* match with the four C2p derived features at 10.3 (15.3), 8.8 (13.8), 7.1 (12.1), and 6.3 (11.3) eV binding energy as observed for 1-cyclohexyl-12-dodecanethiol films.[18] Features *1*−*3*, between 6.0 and 3.5 eV BE, respectively, largely arise from the Au5d emission. This contribution is found to significantly vary as a function of the excitation photon energy, as has been discussed elsewhere.[18] The small plateau near the Fermi energy arises from Au 6s and 6p valence bands.

To identify the spectral features of the individual RazoC10 SAMs, we display photoemission spectra for CH_3azoC10 and CF_3azoC10 in Figure 5. For CF_3 both high- and low-density data are shown, i.e., for 100% and 30% CF_3azoC10 SAMs. Spectra were obtained for 75 eV photons, at $\Psi_i = 83°$ and Θ_e

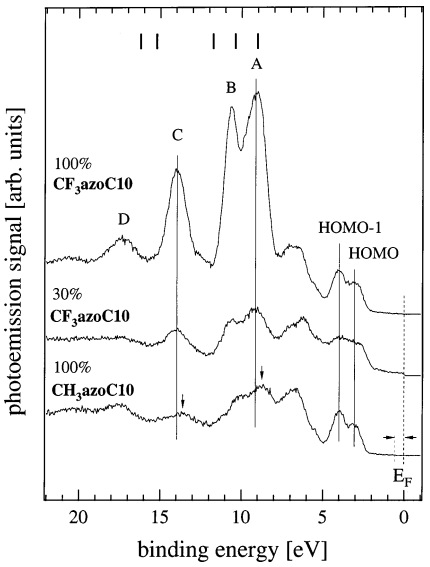

Figure 5. Photoelectron spectra from 100% CH_3azoC10 SAM (bottom), 30% CF_3azoC10 SAM (center), and 100% CF_3azoC10 SAM (top). The spectra were obtained for 83° photon incidence and normal (0°) emission, using 75 eV photons. The bottom spectrum is shifted by −0.45 eV (see text). Labels *A*−*D* refer to peaks that largely arise from fluorine emission (from CF_3). HOMO and HOMO-1 are the highest and second highest occupied molecular orbitals of the azobenzene moiety, respectively. The upper labels in the figure mark the fluorine-derived energies as obtained from the literature (see text).

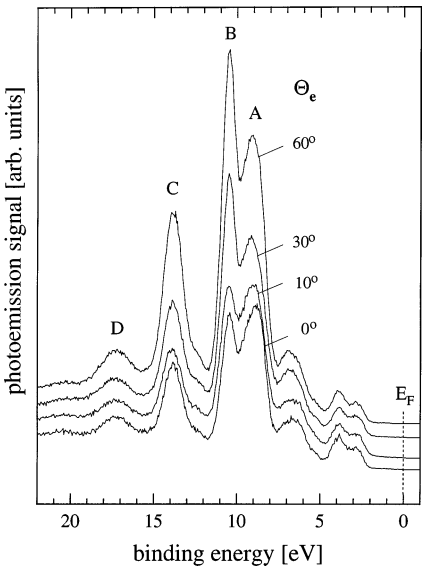

Figure 6. Photoemission spectra from 100% CF_3-azobenzene-terminated alkanethiol SAM obtained for different polar angles, Θ_e, at $h\nu = 75$ eV. The photon incidence angle was 83°. Each spectrum represents a single sweep sampled from a nonexposed surface spot. Spectra have been normalized to the HOMO and HOMO-1 signal of the azobenzene moiety. Peak labels are the same as in Figure 5.

= 0°. All spectra in the figure were obtained for *single* sweeps (see discussion below). For clarity the spectra are vertically displaced. Notice that the CH_3azoC10 spectrum has been shifted by 0.45 eV toward higher BE, as indicated in the figure, to align the organic derived features. The origin of this shift will be addressed in section 3.3.

Comparing the 100% CH_3azoC10 photoemission spectrum (Figure 5 bottom spectrum) with the dodecanethiol spectrum in Figure 4, the attenuation of the Au 5d bands (features *1*−*3*) and of the gold E_F signal due to the larger film thickness can clearly be seen. In this region, two pronounced peaks evolve at 3.1 and 4.0 eV BE. From quantum chemical calculations[20] these features are assigned to the HOMO and HOMO-1 of the azobenzene moiety, respectively. Also the C2p derived features *6-8* become more pronounced, and a previously unresolved feature emerges as a distinct peak at 17.2 eV. These changes identify the photoemission contributions from CH_3-azobenzene units. C2s and C2p peak positions generally differ for CH_3-azobenzene and the pure thiol chain as their orbital energies are not identical.

Comparing the 100% RazoC10 samples, for R = CF_3 vs CH_3, any difference in the photoemission spectra should be mainly due to the different contributions from the two types of tail groups R, because both films are assumed to have identical structures and densities in the trans configuration. For binding energies smaller than 8 eV, and also for energies larger than 16 eV, the two spectra are nearly identical. These energy regions include C2s as well as C2p contributions from the alkyl and the azobenzene parts. Thus the intense new features appearing in the top spectrum (100% CF_3azoC10) in the 8−16 eV energy range are assigned to trifluoromethyl; however, C- and F-derived peaks strongly overlap in this region. In fact, peak positions differ by about 0.4 eV as indicated by the vertical arrows in the figure. The labels *A*−*D* in the figure are introduced to emphasize that the corresponding features mainly arise from CF_3. As inferred from the relative signal intensities in Figure 5, the fluorine contribution to feature *D* is about 50%, while for the former three peaks the fluorine signal makes up for more than 70%. There may be also some CF_3 signal contribution near 6−7 eV binding energy features. To our knowledge, orbital binding energies for CF_3-functionalized benzene or related compounds have not been reported, but our assignment would be fairly consistent with binding energies reported for oriented thin films of *n*-$CF_3(CF_2)_{22}CF_3$,[21] the respective values being indicated in the top of Figure 5. The F2p lone pair orbital is reported at 15.2 and 16.7 eV, and features derived from C−F bonds are found at 18.0, 21.5, and 22.5 eV binding energies.[21] These values are with respect to the vacuum level, which has been accounted for in Figure 5. Notice that the indicated positions are therefore shifted in order to reasonably match our data. Furthermore, semiempirical quantum mechanical calculations (AM1) of CF_3azoC10 confirm that molecular orbitals localized mostly on the CF_3 moiety appear in the same energy range, where we observe strong peaks in PES.[20]

One reason for the strong contribution of the trifluoromethyl to the PE spectrum is its very surface location (see Figure 2), but the main effect is the approximately eight times larger F2p photoionization cross-section. At 75 eV the values for F2p, C2s, and C2p are 3.99, 0.60, and 0.39 Mb/atom,[22] respectively. Qualitatively, the 30% CF_3azoC10 film spectrum (Figure 5) closely resembles the one of 100% CF_3azoC10, only the CF_3-derived features' intensities being decreased. This correlates with the corresponding intensity differences observed in the XPS spectra (see Figure 3).

Angle-resolved photoemission has been measured for 100% CF_3azoC10 samples in order to corroborate the films' structural order. The spectra, Figure 6, were obtained for single scans, each from a pristine surface spot, using 75 eV photons at Ψ_i = 83° incidence, but for different polar emission angles, Θ_e. The spectra were normalized to the HOMO and HOMO-1 intensities of the azobenzene moiety as these features contain no fluorine contribution. Gold substrate contributions to the spectra are insignificant (less than 10% of peak A; compare Figure 5). Large (differential) intensity increases are observed for CF_3-derived

features as Θ_e is being varied from 0° (normal emission) to 60°. The most striking result of Figure 6 is the relative intensity change between peaks *A* and *B*. Angles larger than 60° were not accessible in the present experiment. No Φ dependence of the spectra was found as expected for random azimuthal orientation of molecular domains. Peaks *B* and *C*, which contain the strongest fluorine contribution (see above), increase by almost a factor of 2.5, and peak *A* by a factor of 1.8 from 0° to 60° emission angle. Smaller emission signal increase is observed for feature *D*, but also for the peak near 6.5 eV, both having less CF_3 contributions. This CF_3 signal dependence may be partly attributed to the increased surface sensitivity of photoemission spectroscopy at higher takeoff angles.[23] In addition, one probably needs to invoke symmetry effects, which are not necessarily related to the overall molecular order but rather to the tail group's orbital symmetry, and hence to selection rule arguments. This might explain the differential behavior of the various CF_3 peaks. However, this issue is out of reach at this point.

3.2. Synchrotron Irradiation Effects on Photoemission Spectra. Generally, intense synchrotron irradiation may induce chemical modifications or degradations of the organic sample, which cause the photoemission spectra to change as a function of exposure time. The data presented here so far have been obtained using a low photon flux in single scans. Obviously, studying optical switching of the molecules by photoemission is possible only if any synchrotron light-induced effects are either negligible or separable from the optical excitation.

To obtain insight into the nature of synchrotron radiation-induced changes of the photoemission spectra, we have measured photoemission from 100% and 30% CF_3azoC10 films as a function of the synchrotron exposure time. The experiments were performed at low synchrotron exposure times using photon fluxes $< 1 \times 10^{10}$ 1/s $\times$ 0.1A. These conditions still warrant reasonable count rates for single sweeps. The effect of the synchrotron exposure time on the evolution of the photoemission spectra from a 100% CF_3azoC10 SAM using 75 eV photons is presented in Figure 7. The top spectrum represents the first scan from a film surface spot that had not been previously exposed to synchrotron radiation. The acquisition time for *one* single scan was 30 s. The following two spectra in the figure have been obtained for the second and the third scan (as labeled) for the identical surface spot. Finally, the bottom spectrum has been accumulated over 10 scans (7th to 17th sweep), again from the same spot. Spectra have been normalized to the ring current. The peak assignment is the same as in the previous figures. Notice that the gold Fermi edge is barely seen in the spectra (dashed line) due to the efficient attenuation of substrate signal. The main effect in Figure 7 is the intensity decrease of all CF_3-related peaks, *A*−*D*, with respect to purely alkanethiol- and azobenzene-derived features, for increasing synchrotron exposure time. For the third scan, the intensity drops to ca. half of the initial intensity. At higher exposure (bottom) the features in the < 18 eV binding energy range are smeared out and only minor intensity changes are observed for any of the other features. Furthermore, features containing emission from CF_3 are shifted toward higher binding energies, by up to 450 meV for maximum exposure. No energy shift is observed for any pure alkanethiol- or azobenzene-derived feature. The reason for the CF_3 signal decrease in the spectra will be partly attributed to changes of the orientation of the azobenzene group (see section 3.3). However, the massive signal reduction for high synchrotron light exposure must have further reasons. Eventually molecules may be partially destroyed, which may be accompanied by loss of molecular order. The latter would be consistent with the observed peak broadening. The absence of extra radiation-induced emission features could, in fact, be an indication for insignificant molecular fragmentation. Notice also that the data in Figure 7 provide no evidence for removal of molecules as judged by the constant substrate photoemission signal; however, the possibility of C−F bond cleavage cannot be excluded. Qualitatively similar results have been obtained for the low-concentration azobenzene-CF_3 film (not shown). Energy shifts are up to 400 meV, and the relative intensity decrease of CF_3-derived features is very similar to the 100% CF_3azoC10 case.

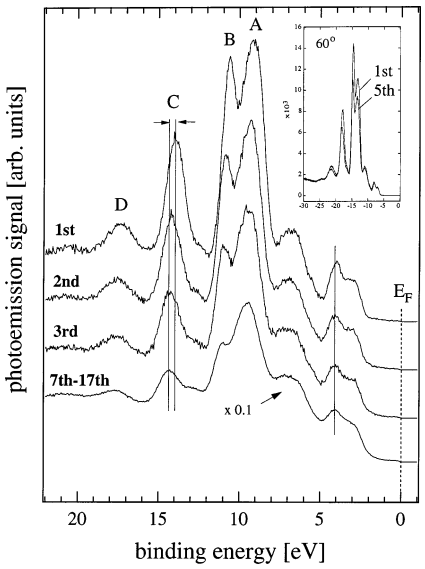

Figure 7. Dependence of photoemission spectra from 100% CF_3-azobenzene-terminated alkanethiol SAM on the synchrotron light exposure. $h\nu = 75$ eV, 83° photon incidence, and normal emission. The exposure time is given by the number of sweeps (from the identical surface spot). Data are normalized to the ring current. Labels *A*−*D* refer to peaks largely composed of fluorine signal. The inset compares the photoemission spectra for the 1st and 5th scan at 60° polar emission angle. Spectral shifts associated with a change of the CF_3-azobenzene dipole are indicated.

Apparently, synchrotron-induced effects have to be well accounted for if one attempts to assign changes of the photoemission spectra that are induced by laser photoisomerization. Moderate synchrotron light exposure, corresponding to about 3−5 sweeps under the present experimental conditions, does not lead to a loss of spectral resolution, but relative peak intensities may be affect. This could be an indication of synchrotron light-induced sample modifications, in terms of a (collective) change of the molecular orientation, which largely maintains the films' molecular order. In particular, the inset in Figure 7 demonstrates that for suitably chosen exposure the photoemission spectra tend to become very similar to spectra for nonexposed samples, measured at a *different* emission angle. For example the photoemission spectrum of an exposed film at 60° (obtained for the 5th scan; inset Figure 7) and the spectrum of a nonexposed surface spot at 30° (Figure 6), for the first scan, are nearly identical. The result would be consistent with a well-defined inclination of the CF_3 groups relative to the surface normal, induced by synchrotron radiation. A further discussion will be presented along with the changes observed for laser-excited films in the next paragraph, as they appear to be of related nature.

3.3. 360 nm Laser Excitation. The as-prepared RazoC10 SAMs investigated here are assumed to be in the thermody-

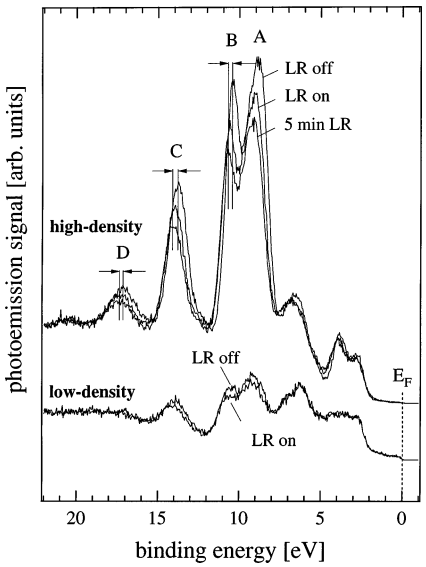

Figure 8. Laser-induced changes of the photoemission spectra for two azobenzene-CF_3-terminated alkanethiol SAMs. *A*−*D* denote peaks largely composed of fluorine signal. Top panel: effect of time-correlated 360 nm laser pulse and of 5 min laser exposure prior to recording the photoemission spectra of a 100% CF_3azoC10 film. Bottom panel: laser on vs off for the 30% azobenzene-CF_3-terminated alkanethiol SAM. The spectra were obtained for *one* single sweep from a nonexposed surface spot. $h\nu = 75$ eV, $\Psi_i = 83°$, and $\Theta_e = 0°$.

namically more stable trans configuration,[3,4] in agreement with a recent STM study on hexyl-azobenzene SAMs.[13] We have shown above that for suitably low synchrotron photon flux the photoemission spectra, in fact, represent the electronic structure of intact trans R-azobenzene-alkanethiol. Longer synchrotron exposure considerably alters the photoemission features (section 3.2.). Hence, combined laser and synchrotron pulse experiments had to be performed at low *total* synchrotron light exposure. In the top of Figure 8, we present photoemission spectra from 100% CF_3azoC10 obtained for dark and laser-excited samples using 360 nm photons. The laser power at the sample was about 10 mW/cm^2. Each PE spectrum has been obtained for one single scan from a nonexposed surface spot using 75 eV photon energy at $\Psi_i = 83°$ and $\Theta_e = 0°$. The spectra in the figure have been superimposed, as this best shows the differences induced by the laser. For the laser-pumped sample (labeled LR on) ca. 15% lower photoemission intensities are observed in the spectra, particularly for peaks *A* through *D* as compared to the dark sample (labeled LR off). Furthermore, the same features exhibit differential peak shifts to higher binding energy, by 150−250 meV. Interestingly, the HOMO and HOMO-1 features broaden, but they experience almost no shift (<50 meV). The gold substrate features, as well, remain fixed at the same binding energy. Also shown is the spectrum from a surface spot, which has been exposed to laser irradiation for five minutes directly prior to the photoemission measurement. Qualitatively, the spectral changes are identical as compared to the ones observed for synchronized laser pulses; however, the intensity changes and the energy shifts (200−400 meV) are more pronounced for the preexposed sample. No further changes have been observed for laser exposures up to 30 min prior to recording the photoemission spectra. The bottom pair of photoemission spectra in Figure 8 show the corresponding data for dark and laser-excited 30% CF_3azoC10 SAMs. The results are qualitatively identical to the 100% CF_3azoC10 case, but the changes are less pronounced. The maximum energy shift is about 100−150 meV.

Both the decrease of emission intensity from trifluoromethyl-related molecular orbitals (MOs) and the shift of certain emission features toward higher binding energy upon laser excitation are consistent with the trans−cis isomerization of CF_3azoC10. The former may be attributed to the partial burial of the CF_3 moiety. As shown schematically in Figure 2, for the cis conformation, the CF_3 moiety is inclined toward the surface. Hence, depending on the actual tilt of the alkanethiol (the ca. 30° angle shown in Figure 2 is likely to be an upper limit) the CF_3 group gets less exposed at the surface. Given the surface sensitivity of photoemission spectroscopy, this directly translates into a signal drop from this group due to the relatively stronger attenuation of emission features *A*−*D*. At the same time, symmetry arguments may be responsible for the lower intensity observed during laser excitation, but as noted earlier in the discussion of angle-dependent spectra, we cannot at present elaborate on this issue further.

Also the energy shifts are a consequence of the molecular structural change, as the latter is associated with a change of the total dipole moment of the molecule. Notice that sample *charging* can be ruled out as the cause of the observed shifts. Charging is unlikely to occur for a monolayer system on a conductive substrate, and furthermore charging-compensation in the presence of additional laser irradiation would in fact cause a spectral shift in the opposite direction,[24] i.e., to lower binding energy. The strong electron withdrawing character of CF_3 gives rise to a permanent dipole moment (m) extending across the entire CF_3-azobenzene moiety. As sketched in Figure 2, the dipole is aligned almost parallel to the long axis of the azobenzene chromophore in trans conformation. The positive charge is close to the alkoxy moiety, while the negative part of the surface dipole points toward the vacuum side. For the cis form, the dipole moment is smaller and further tilted away, by ca. 26°, relative to the alkylthiol main axis. On the basis of semiempirical quantum mechanical calculations (PM3) absolute values of the dipoles have been calculated to be $m = 4.6$ D for trans, and 3.9 D for cis, respectively.[4] The lower and upper limits for the change of the dipole component perpendicular to the surface ($\Delta m_\perp$) are estimated to be 1.1 and 1.8 D per molecule, respectively. The limits are imposed by the relative orientation of the azobenzene moiety relative to the substrate normal. The lower bound corresponds to the long *trans*-azobenzene molecular axis being perpendicular to the substrate surface (i.e., 30° alkylthiol tilt), and the upper bound refers to the alkylthiol axis being perpendicular to the surface (compare Figure 2). No proximity effects of the gold surface have been accounted for in our calculations, and also the dipole moment of the gold−alkylthiol system has been neglected.[25,26]

The change of the samples' work function, $\Delta\phi$, which correlates with the change of the normal dipole component, can be estimated by means of the Helmholtz equation $\Delta\phi = q \cdot n \cdot \Delta m_\perp/\epsilon_r\epsilon_0$.[27] Here, q denotes the elementary charge, n is the number of dipoles per unit area, ϵ_r the relative dielectric constant, and ϵ_0 is the vacuum permittivity. In photoemission spectroscopy, $\Delta\phi$, leads to a shift of the measured binding energy (relative to E_F) of an emission feature from a certain MO, but only if the corresponding MO is localized *above* or *within* the dipole. Any emission feature from states *below* the dipole is not affected, that is, it remains at the same BE. To illustrate the effect, we show in Figure 9 a schematic energy level diagram of the sample representing the relevant energies before (trans) and after (cis) isomerization. This simple model would be consistent with the experimental differential shifts, which are largest for CF_3-derived features (*A*−*D*), this group being

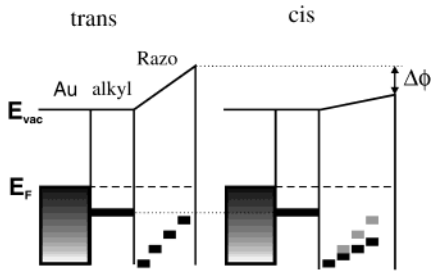

Figure 9. Schematic energy level diagram of a CF_3azoC10 molecule on the Au surface in the trans (left) and cis (right) conformation. E_F denotes the Fermi level, E_{vac} is the vacuum level. Razo denotes the azobenzene part that forms the dipole. Individual MOs are indicated by black bars, gray bars in the right figure mark the positions of these MOs before isomerization. $\Delta\Phi$ is the local work function change resulting from the trans−cis transformation.

localized at the outermost part of the molecules. Even though this is in qualitative agreement with our observations, a more advanced model would be required to account for all the experimental findings. For instance, it is not obvious what causes the spectral shift in the case of $R = CH_3$ in Figure 5. Notice that this issue is independent of photoisomerization. Furthermore, as not all molecules will be switched (see below), one would expect a distribution of measured binding energies of a given MO leading to a certain peak broadening. No clear evidence for such an effect has been inferred in the present experiments. Possibly the broadening is masked by the lateral extension of the surface dipole and the resulting *mean* work function.

Using the Helmholtz equation (see above) we can estimate the number of switched molecules per unit area. An, admittedly rough, estimation of the fraction of molecules that have switched after optical excitation is given in the following. With $\Delta m_\perp$ either 1.1 or 1.8 D, and setting ϵ_r at either 3, which is a commonly accepted value for conjugated organic materials,[28] or 1 (accounting for the vacuum interface), and taking an average shift of feature *A* in Figure 8 (300 meV), one obtains for the upper and lower limit $n = 4 \times 10^{13}$ cm^{-2} and 1.8×10^{14} cm^{-2}, respectively, for the present experimental conditions. This compares to 3.5×10^{14} cm^{-2} [29,30] total surface coverage of all-trans species in the initial 100% CF_3azoC10, suggesting that about 10−50% of the molecules in the SAM have switched to the cis configuration after laser excitation. We emphasize that the value for ϵ_r is unknown for our samples, and therefore constitutes the largest uncertainty for the estimation. Our calculated number seems somewhat too large as the footprint area (projected area assuming upright standing alkanethiols) of the molecules in the trans (36 Å^2) vs cis (106 Å^2) conformation would impose considerable steric hindrance. This could also be the reason for the fact that the energy shifts observed for the 100% vs 30% film do not scale proportionally with the CF3azoC10 density. In fact, Kelvin probe measurements suggest an optimum switching capability near 30% mix.[4]

Comparing the changes in the photoemission spectra as a function of laser versus synchrotron exposure time, only subtle differences are observed with respect to both peak shifts and intensity variations. The net total change of the spectra is thus determined by the sum of laser *and* synchrotron light exposure and, at least for relatively low exposure, laser and synchrotron irradiation produce similar spectral changes. For longer exposure, spectral changes become more pronounced if induced by high-energy photons. For instance, the photoemission spectrum for the third scan in Figure 7 shows a broader and less resolved structure as compared to the 5 min laser exposure spectrum shown in Figure 8. It seems that VUV synchrotron radiation also induces trans−cis isomerization, as does the laser radiation, yet these two excitation sources differ in terms of their efficiency. Furthermore, photodegradation contributions might have to be accounted for as well. The effect of long-time laser exposure on the spectra was found to saturate after a few minutes, which is consistent with our expectations that the maximum number of molecules has been switched. The time constant for this process has been shown to be on the 100 s time scale.[3,4]

Summary

We have reported photoemission spectra from CF_3-azobenzene-terminated alkanethiol SAMs with emphasis on the photoinduced trans-to-cis isomerization of the azobenzene unit. It has been concluded that VUV photoemission may be applied for investigating isomerization processes in azobenzene alkanethiol SAMs only if the competitiveness of laser and synchrotron photon-induced processes is correctly taken into account. This has been inferred by systematically studying the effect of extended irradiation of the samples by both laser and synchrotron light on the photoemission spectra. Photon-induced binding energy shifts and photoemission intensity changes have been attributed to the change of the molecular orientation and dipole moment relative to the substrate surface, associated with the two isomeric configurations. Clearly, further investigations are required in order to obtain detailed information on the nature of the photoprocesses. This would include the variation of the tail group and the systematic variation of the SAM free volume. However, most importantly, photoemission spectra need to be measured for laser-pumped films for both wavelengths 360 and 450 nm to reverse the transformation. We propose that shifting the trans/cis photostationary ratio of the molecules by suitable UV vs visible irradiation is possible, and thereby synchrotron photon-induced effects could be actively compensated. Further studies in this direction are in progress.

References and Notes

(1) Ulmann, A. *An Introduction to Ultrathin Films*; Academic Press: San Diego, CA, 1991.

(2) Mutsuyoshi, M.; Terrettaz, S.; Tachibana, H. *Adv. Colloid Interface Sci.* **2000**, *87*, 147.

(3) Stiller, B.; Karageorgiev, P.; Perez-Enciso, E.; Velez, M.; Vieira, S.; Reiche, J.; Knochenhauer, G.; Prescher, D.; Brehmer, L. *Surf. Interface Anal.* **2000**, *30*, 549.

(4) Stiller, B.; Karageorgiev, P.; Jüngling, T.; Prescher, D.; Zetzsche, T.; Dietel, R.; Knochenhauer, G.; Brehmer, L. *Mol. Cryst. Liq. Cryst.* **2001**, *355*, 401.

(5) Ulman, A. *Chem. Rev.* **1996**, *96*, 1533.

(6) Schreiber, F. *Prog. Surf. Sci.* **2000**, *65*, 151.

(7) Takami, T.; Delamarche, E.; Michel, B.; Gerber, C.; Wolf, H.; Ringsdorf, H. *Langmuir* **1995**, *11*, 3876.

(8) Petrachenko, N. E.; Vovna, V. I.; Furin, G. G. *J. Fluorine Chem.* **1993**, *63*, 85.

(9) Kobayashi, T.; Yokota, K.; Nagakura, S. *J. Electron Spectrosc. Relat. Phenom.* **1975**, *6*, 167.

(10) Brace, N. O. *J. Fluorine Chem.* **1983**, *62*, 271.

(11) Zhang, H.-L.; Zhang, J.; Li, H.-Y.; Liu, Z.-F.; Li, H.-L. *Mater. Sci. Eng. C* **1999**, *8*−*9*, 179.

(12) Han, S. W.; Kim, C. H.; Hong, S. H.; Chung, Y. K.; Kim, K. *Langmuir* **1999**, *15*, 1579.

(13) Tamada, K.; Nagasawa, J.; Nakanishi, F.; Abe, K.; Ishida, T.; Hara, M.; Knoll, W. *Langmuir* **1998**, *14*, 3264.

(14) Stiller, B.; Knochenhauer, G.; Markava, E.; Gustina, D.; Muzikante, I.; Karageorgiev, P.; Brehmer, L. *Mater. Sci. Eng. C* **1999**, *8*−*9*, 385.

(15) Gatzke, J.; Winter, B.; Quast, T.; Hertel, I. V. *SPIE Proc.* Vol. **3464**, pp 14−20, San Diego, 23−23 July 1998.

(16) Winter, B.; Gatzke, J.; Quast, T.; Will, I.; Wick, M. T.; Liero, A.; Pop, D.; Hertel, I. V. *SPIE Proc.* Vol. **3451**, pp 62−69, San Diego, 23−23 July 1998.
(17) Quast, T.; Bellmann, R.; Winter, B.; Gatzke, J.; Hertel, I. V. *J. Appl. Phys*. **1998**, *83*, 1642.
(18) Duwez, A. S.; Di Paolo, S.; Ghijsen, J.; Riga, J.; Deleuze, M.; Delhalle, J. *J. Phys. Chem. B* **1997**, *101*, 884.
(19) Haran, A.; Naaman, R.; Askenasy, G.; Shanzer, A.; Quast, T.; Winter, B.; Hertel, I. V. *Eur. Phys. J. B* **1999**, *8*, 445.
(20) Koch, N.; Winter, B. Unpublished.
(21) Miyamae, T.; Hasegawa, S.; Yoshimura, D.; Ishii, H.; Ueno, N.; Seki, K. *J. Chem. Phys.* **2000**, *112*, 3333.
(22) Yeh, J. J.; Lindau, I. *Atom. Data Nucl. Data Tables* **1985**, *32*, 1.
(23) Wagner, C. D.; Riggs, W. M.; Davis, L. E.; Moulder, J. F.; Muilenberg, G. E. *Handbook of X-ray Photoelectron Spectroscopy*; Perkin-Elmer: Eden Prairie, 1978.
(24) Koch, N.; Pop, D.; Weber, R. L.; Böwering, N.; Winter, B.; Wick, M.; Leising, G.; Hertel, I. V.; Braun, W. *Thin Solid Films* **2001**, *391*, 81.
(25) Ishii, H.; Sugiyama, K.; Ito, E.; Seki, K. *Adv. Mater*. **1999**, *11*, 605.
(26) Campbell, I. H.; Rubin, T. A.; Kress, J. D.; Martin, R. L.; Smith, D. L.; Barashkov, N. N.; Ferraris, J. P. *Phys. Rev. B* **1996**, *54*, R14321.
(27) Christmann, K. *Surface Physical Chemistry*; Steinkopff: Darmstadt, 1991.
(28) Hill, I. G.; Kahn, A.; Soos, Z. G.; Pascal, R. A. *Chem. Phys. Lett.* **2000**, *327*, 181.
(29) Gustina, D.; Markava, E.; Muzikante, I.; Stiller, B.; Brehmer, L. *Adv. Mater. Opt. Electron.* **1999**, *9*, 245.
(30) Zhang, A. D.; Qin, J. G.; Gu, J. H.; Lu, Z. H. *Thin Solid Films* **2000**, *375*, 242.